BIOCHEMISTRY
including biophysical chemistry & molecular biology
Article

Biochemistry **2010,** *49,* 7089–7099 7089
DOI: 10.1021/bi100575s

Lysophospholipid Micelles Sustain the Stability and Catalytic Activity of Diacylglycerol Kinase in the Absence of Lipids†

Julia Koehler,‡ Endah S. Sulistijo,‡,§ Masayoshi Sakakura, Hak Jun Kim,∥ Charles D. Ellis, and Charles R. Sanders*

Department of Biochemistry and Center for Structural Biology, Vanderbilt University School of Medicine, Nashville, Tennessee 37232-8725 ‡These authors contributed equally to this work §Current address: Department of Molecular Biophysics and Biochemistry, Yale University, New Haven, CT 06520-8114 ∥Current address: Korea Polar Research Institute, Incheon 406-840, Korea.

Received April 14, 2010; Revised Manuscript Received July 12, 2010

ABSTRACT: There has been a renewal of interest in interactions of membrane proteins with detergents and lipids, sparked both by recent results that illuminate the structural details of these interactions and also by the realization that some experimental membrane protein structures are distorted by detergent−protein interactions. The integral membrane enzyme diacylglycerol kinase (DAGK) has long been thought to require the presence of lipid as an obligate "cofactor" in order to be catalytically viable in micelles. Here, we report that near-optimal catalytic properties are observed for DAGK in micelles composed of lysomyristoylphosphatidylcholine (LMPC), with significant activity also being observed in micelles composed of lysomyristoylphosphatidylglycerol and tetradecylphosphocholine. All three of these detergents were also sustained high stability of the enzyme. NMR measurements revealed significant differences in DAGK−detergent interactions involving LMPC micelles versus micelles composed of dodecylphosphocholine. These results highlight the fact that some integral membrane proteins can maintain native-like properties in lipid-free detergent micelles and also suggest that C_{14}-based detergents may be worthy of more widespread use in studies of membrane proteins.

Solution NMR[1] and X-ray crystallographic structural studies of purified integral membrane proteins are often carried out in detergent micelle solutions, an imperfect medium given that protein−lipid interactions are sometimes both specific and important to integral membrane protein structure and function (*4*−*7*). Moreover, it is now clear that some high-resolution structures of membrane proteins include micelle-generated distortions (*8*−*11*) and also that the energetics of membrane protein folding and intermolecular interactions can be altered in micelles relative to native-like membrane bilayers (*12*−*14*). This has led to increased use of lipid-containing mixed micelles, bicelles, nanodisks, and other model membranes to better approximate lipid bilayers than detergent-only micelles (*15*−*20*). In this paper, we explore the alternative approach of finding improved detergents for sustaining the native-like stability and function of membrane proteins, without resorting to lipid-containing media.

†This study was supported by NIH Grant RO1 GM47485.

*To whom correspondence should be addressed: E-mail: chuck.sanders@vanderbilt.edu. Phone: 615-936-3756. Fax: 615-936-2211.

[1]Abbreviations: 3-D, three dimensional; ASB-14, 3-[*N*,*N*-dimethyl(3-myristoylaminopropyl)ammonio]propanesulfonate; CL, bovine heart cardiolipin; CMC, critical micelle concentration; CYF7, cyclohexyl-1-heptylphosphocholine; DAG, *sn*-1,2-diacylglycerol; DAGK, diacylglycerol kinase; DBG, *sn*-1,2-dibutyrylglycerol; DHG, *sn*-1,2-dihexanoylglycerol; DIG, digitonin; DM, *n*-decyl β-D-maltopyranoside; DMPC, dimyristoylphosphatidylcholine; DPC, *n*-dodecylphosphocholine; DTAB, dodecyltrimethylammonium bromide; GRA, glycyrrhizic acid; HDPC, *n*-hexadecylphosphorylcholine; LLPC, lysolauroylphosphatidylcholine; LMPC, lysomyristoylphosphatidylcholine; LMPG, lysomyristoylphosphatidylglycerol; LPPC, lysopalmitoylphosphatidylcholine; LPPG, lysopalmitoylphosphatidylglycerol; LS, *n*-lauroylsarcosine; NMR, nuclear magnetic resonance; NOESY, nuclear Overhauser effect NMR spectroscopy; POPC, 1-palmitoyl-2-oleoylphosphatidylcholine; TDPC, *n*-tetradecylphosphorylcholine; TROSY, transverse relaxation-optimized NMR spectroscopy; Trp, tryptophan; Z3-14, Zwittergent 3-14.

Escherichia coli diacylglycerol kinase (DAGK) is well-suited for studies designed to identify optimal detergents. DAGK is a homotrimeric membrane enzyme with nine transmembrane helices and three active sites per trimer that catalyzes direct phosphoryl transfer from MgATP to diacylglycerol to produce phosphatidic acid. In pioneering early work, the laboratories of Kennedy, Bell, and Sandermann showed that DAGK does not exhibit significant catalytic activity in micelles formed by common detergents unless lipid is added (*21*−*25*). These early studies suggested that lipids play a cofactor role in support of DAGK catalysis. However, the range of commercially available detergents has dramatically expanded since those studies were carried out. The structure of DAGK was recently determined in DPC micelles using NMR spectroscopy (*26*), conditions in which DAGK retains considerable catalytic activity, but only at very high substrate concentrations as a consequence of dramatically elevated substrate K_m. This latter fact prevents structural studies of DAGK in DPC micelles under conditions in which it is saturated with its substrates or products. Here we reexplore detergent space to see if surfactants are now available that can sustain native-like DAGK structure, stability, and catalysis. It is shown that certain C_{14} chain detergents are able to do so, with the lysophospholipids proving especially effective.

EXPERIMENTAL PROCEDURES

Materials. Detergents and lipids used in this study were purchased from Anatrace (Maumee, OH), Avanti (Alabaster, AL), Sigma (St. Louis, MO), or Calbiochem (San Diego, CA). The diacylglycerols dibutyrylglycerol (DBG) and dihexanoylglycerol (DHG) were synthesized in-house as described previously (*3*).

© 2010 American Chemical Society
Published on Web 07/16/2010

Expression and Purification of DAGK. The gene that encodes N-terminal His_6-tagged wild-type *E. coli* DAGK was ligated into the pSD005 plasmid (*3*, *27*), which was then transformed into *E. coli* WH1061 cells. WH1061 is a leucine auxotroph strain that does not express endogenous DAGK (*28*). DAGK was expressed in isotopically labeled form and then purified to the point where it is a pure protein attached to Ni(II)-chelate resin bathed in a buffer containing 1.5% (v/v) Empigen BB detergent (Sigma, St. Louis, MO), 40 mM HEPES, 300 mM NaCl, and 40 mM imidazole, pH 7.5, essentially as described elsewhere(*26*, *29*, *30*). Empigen BB was then exchanged out for the detergent of interest (e.g., LMPC) by passing 10 column volumes of 25 mM sodium phosphate buffer (pH 7.2) containing the test detergent through the column. Finally, DAGK was eluted from the column with 250 mM imidazole solution (pH 7.8) containing the same test detergent. The amount of DAGK in the elution fractions was determined spectrophotometrically based on an extinction coefficient of 2.18 $(mg/mL)^{-1}$ cm^{-1} at 280 nm.

Measurement of DAGK Activity. The activity assay is derived from protocols that have been described previously (*3*, *31*) whereby DAGK-catalyzed phosphoryl transfer from MgATP to DAG is coupled to NADH oxidation by pyruvate kinase (PK) and lactate dehydrogenase (LDH, Sigma) at 30 °C. The relatively short-chained dibutyrylglycerol (DBG) and dihexanoylglycerol (DHG) were the forms of diacylglycerol used in these studies because of their reasonably high solubility in detergent solutions (*3*, *32*). The pH 6.9 activity assay mix was composed of 75 mM PIPES, 50 mM LiCl, 0.1 mM EGTA, 0.1 mM EDTA, 1 mM phosphoenolpyruvate (Sigma), 3 mM MgATP (Sigma), 0.25 mM NADH (Sigma), 12 mM magnesium acetate, and 7.8 mM DBG. For the standard mixed micellar assay, this mixture also contained the detergent DM (at 21 mM, 19 mM of which is micellar) and the lipid cardiolipin (CL, from beef heart, at 0.66 mM, which corresponds to 3 mol %). For other assays, DM and CL were replaced with the detergent of interest. DAGK stocks were prepared by diluting the purified protein to a concentration 0.15 mg/mL using detergent-containing elution buffer. Aliquots of this stock were added to the activity assay mix that had been equilibrated with PK and LDH (14 and 20 units, respectively, per milliliter of mix). The decrease in absorbance at 340 nm resulting from NADH oxidation (as coupled to the DAGK reaction) was monitored spectrophotometrically, with the slope being converted to units of DAGK activity (1 unit = 1 micromole of DAG phosphorylated per minute) using the extinction coefficient for NADH of 6110 M^{-1} cm^{-1}.

Activity data for determination of steady-state kinetic parameters V_{max} and K_m were collected using the same methods described above, with the exception that in each analysis the concentration of one substrate was varied (0−8 mM MgATP or 0−25 mM DBG) while the other substrate was held constant at a near-saturating level (20 mM for DBG and 3 mM for MgATP). The measured rates were plotted as a function of variable substrate concentrations and fit by the Michaelis−Menten equation (with a Hill coefficient being applied to the variable substrate concentration) using the Solver module in Microsoft Excel.

Thermal Stability of DAGK. Purified DAGK was diluted to a concentration of 0.1 mg/mL using elution buffer plus detergent at either pH 7.8 or pH 6.5. Samples were incubated at 45 and 70 °C, and aliquots were withdrawn at various time points, rapidly frozen in liquid N_2, and then stored at −80 °C. Samples were later thawed and subjected to the standard DM/CL/DHG mixed micellar DAGK activity assay to determine the levels of remaining DAGK activity.

Circular Dichroism Spectroscopy. Samples for CD spectroscopy were prepared by removing imidazole from purified DAGK using a PD-10 desalting column (GE Healthcare) equilibrated with buffer containing 100 mM sodium chloride, 20 mM sodium phosphate, pH 6.5, and the test detergent of interest. For acquisition of CD spectra, DAGK was diluted using desalting buffer to 50−60 μM for near-UV CD spectroscopy or to 10−12 μM for far-UV CD spectroscopy.

CD experiments were carried out using a Jasco J-810 instrument equipped with a Peltier temperature control, and the samples were placed in either 1 cm (near-UV) or 0.1 cm (far-UV) path length quartz cuvettes. CD spectra were acquired at 5 °C increments between 20 and 80 °C, with 1 min of equilibration prior to each acquisition. The far-UV CD spectra were acquired between 190 and 260 nm with 1 nm bandwidth, while the near-UV spectra were acquired from 250 to 350 nm with 1 nm bandwidth. Baseline spectra were acquired for the protein-free desalting buffers and subtracted from the spectra of protein-containing samples. For all acquisitions three spectra were collected and averaged to give the final trace.

The K2D algorithm (http://www.embl.de/~andrade/k2d.html) was used to calculate secondary structure from far-UV CD spectra.

NMR Spectroscopy of DAGK. ^{15}N-Labeled DAGK was purified using the protocol described above. When the protein was purified into LMPC and DPC, D_2O and EDTA were added to 10% and 0.5 mM, respectively, and the sample was concentrated using centrifugal ultrafiltration (Millipore Ultracel, 10 mL, 10 kDa cutoff), and then transferred to an NMR tube. For the protein in TDPC and LMPG the pH 7.8 purification buffer containing 250 mM imidazole (pH 7.8) was exchanged for a pH 6.5 10 mM Bis-Tris buffer by repeated centrifugal ultrafiltration/redilution cycles. The completeness of the exchange was monitored by checking the pH of the filtrate. EDTA and D_2O were added to all samples to a final concentration of 0.5 mM and 10% (v/v). For DAGK in TDPC and LMPG magnesium chloride was also added to 2 mM.

2D ^1H,^{15}N-TROSY NMR spectra (*33*) were acquired at 45 °C using a Bruker 800 MHz Avance spectrometer equipped with a triple resonance cryoprobe. The Weigelt version of the TROSY experiment was used (*34*). Data were processed using NMRPipe/NMRDraw software (*35*) and analyzed using SPARKY 3 (T. D. Goddard and D. N. Kneller, University of California, San Francisco).

3-D $^1H-^{15}N$ NOESY-TROSY (*36*, *37*) spectra were acquired at 800 MHz and 45 °C. $^1H-^{15}N$ NOESY-TROSY spectra were acquired at 800 MHz field. For DAGK dissolved in LMPC micelles, a pulse scheme reported by Zhu et al. (*38*) was used. The spectrum was acquired with 99 complex points and an acquisition time of 8.87 ms in the indirect ^1H dimension, 24 complex points and an acquisition time of 9.25 ms in the ^{15}N dimension, and 1024 complex points and an acquisition time of 91.8 ms in the ^1H observe dimension with 24 scans. The mixing time and the delay for relaxation between scans were 150 ms and 1.1 s, respectively. For DAGK in DPC micelles, a pulse scheme based on the method designed by Schulte-Herbruggen(*39*) was used. The spectrum was acquired with 128 complex points and an acquisition time of 16.3 ms in the indirect ^1H dimension, 64 complex points and an acquisition time of 25.88 ms in the ^{15}N dimension, and 1024 complex points and an acquisition time of 91.8 ms in the ^1H

Table 1: Activity Levels of DAGK Assayed in Various Detergent Conditions

detergent	detergent class	concn (%, w/v)	DAGK activity (units/mg) when small aliquots of DM/DAGK stock solutions were used to initiate assay	DAGK activity (units/mg) when assays were initiated with DAGK stocks in the same detergent as used in assay
LLPC	lyso-PC	0.5	ND[a]	18 ± 6
LMPC	lyso-PC	0.2	66	83 ± 7
LPPC	lyso-PC	0.2	ND	44 ± 2
LMPG	lyso-PG	0.2	22	19 ± 3
LPPG	lyso-PG	0.2	ND	6.6 ± 5
DPC	alkylphosphocholine	0.5	0.1	0.3
TDPC	alkylphosphocholine	0.2	28	10 ± 1
CYF7	alkylphosphocholine	0.5	~0	ND
Z3-14	zwitterionic	0.2	~0	ND
ASB-14	zwitterionic	0.2	0.6	ND
LS	anionic	2.0	~0	ND
DTAB	cationic	0.5	~0	ND
DM	nonionic	0.5	0.3	ND
GRA	saponin	2.0	~0	ND
DM/CL[b]	mixed micelles		16	ND
DMPC[c]	lipid vesicles		63	ND
POPC[c]	lipid vesicles		52	ND

[a]ND: not determined. [b]While the activity of DAGK in DM/CL (ideal mixed micelles for DAGK) can reach 100 units/mg when saturating DHG is used as the lipid (diacylglycerol) substrate, the conditions used for obtaining the data of this table involved the use of DBG as the lipid substrate at a concentration that is subsaturating even for DAGK in DM/CL. This was to avoid problems with solubility and stability for some detergents and assay components that can result from the high concentrations of diacylglycerol. Thus, the observed < 100 units/mg activity under DM/CL conditions reflects the fact that DAGK is not saturated with its DAG substrate under these conditions. [c]From ref *3*.

observe dimension with 8 scans. The mixing time and the delay for relaxation between scans were 100 ms and 1.3 s, respectively.

RESULTS

C14-Based Detergents Show Promise for Biochemical Studies of DAGK. While the activity of purified DAGK is generally low in a variety of lipid-free micelles (*21*, *22*, *25*, *32*, *40*), some data have suggested that DAGK is more active in longer chain detergents relative to shorter chain detergents (*41*). We therefore screened for detergents that are able to sustain DAGK's activity even in the absence of added lipids, with a particular emphasis on detergents that are lipid-like in terms of having relatively long C_{14} alkyl chains. Detergents tested included nonionic, ionic, zwitterionic, lysophospholipids, and sterol-based detergents, each of which was first verified not to hinder the DAGK assay reaction coupling system. These assays were initially carried out by adding small aliquots of DAGK stock solutions prepared in DM micelles (to far below the DM's CMC) into assay mixtures containing the test detergent at concentrations well above the same detergent's CMC. Results for this screen are given in Table 1. DM/CL detergent/lipid mixed micelles that are known to sustain native-like DAGK activity (*3*) were used as a positive control for this screen. It was observed that when solubilized in the C_{14}-based TDPC and lysophospholipids (LMPG and LMPC), DAGK exhibited activity that matched or exceeded its DM/CL control activity, whereas in all other cases the activity was much lower reflecting either a very low V_{max} for catalysis and/or of grossly elevated substrate K_m. The C_{14} chain detergents ASB-14 and Z3-14 failed to support catalysis, indicating that having a C14 chain is not the only factor that determines detergent efficacy.

The fact that TDPC, LMPC, and LMPG support considerable DAGK activity depends in part on their C_{14} chains. Activities were measured for DAGK prepared in the corresponding C_{12}- and C_{16}-based compounds as summarized in the final column of Table 1. For these tests, DAGK was directly purified into each of the detergents and then assayed in a mixture containing the same detergent. For all three classes of detergents, the C_{14} compound yields the highest activity within each class, with the lyso-PC compounds exhibiting higher activities than the corresponding alkyl-PC or lyso-PG compounds. Together, these data suggest that significant DAGK activity can be supported by detergents that have both C_{14} chains and suitable headgroups.

LMPC Micelles Yielded the Most Favorable Steady-State Kinetic Parameters. We determined V_{max} and K_m for DAGK and its substrates diacylglycerol and MgATP in LMPC, LMPG, and TDPC. Rates were measured at varying concentrations of one substrate while the other substrate was maintained at a near-saturating concentration. The C4-chain DBG was used as the diacylglycerol substrate because it can be employed at high (saturating) concentrations unlike longer chain forms of DAG, which tend to either form oil droplets or induce precipitation of assay components before saturating concentrations can be reached.

Figure 1 shows the kinetic data for DAGK in LMPC, LMPG, and TDPC micelles. In each case, the data are slightly sigmoidal, exhibiting a lag phase at low substrate concentrations suggesting deviation of DAGK from ideal Michaelis−Menten behavior. The origin of this phenomenon could be related to the fact that DAGK is homotrimeric, with each of its three active sites being shared between subunits, although this is not the only possible explanation. Because of this apparent cooperativity, we applied a Hill coefficient to fit the Michaelis−Menten equation to the data, with results given in Table 2. For both substrates, the Hill coefficients determined in all cases indicate positive cooperativity. For LMPG and LMPC the V_{max} determined when MgATP was varied (at fixed DBG concentration) was slightly less than when the concentration of DBG was varied (with fixed MgATP). This reflects the fact that the fixed concentration of MgATP was closer to saturation than was fixed DBG. This was not the case

for TDPC because K_m for MgATP is elevated 3-fold in that detergent.

The kinetic parameters of Table 2 confirm that DAGK is most efficient in LMPC micelles. The values for the apparent V_{max} and K_m are comparable to those observed for DAGK under ideal mixed micellar conditions (*27*, *31*, *42*), which are similar to those seen for DAGK in vesicles (*3*, *43*, *44*). DAGK's catalytic properties in both LMPG and TDPC are less ideal than in LMPC but are still impressive.

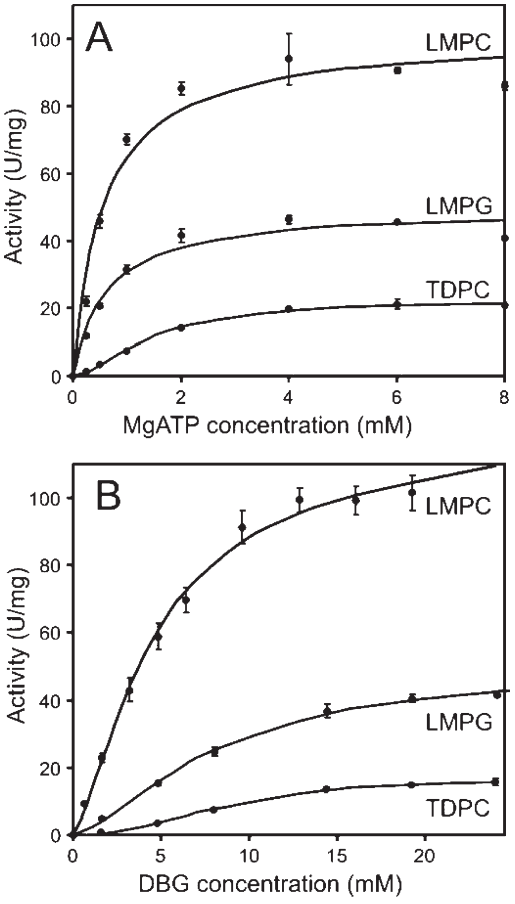

FIGURE 1: Steady-state kinetic analysis of DAGK in TDPC, LMPG, and TDPC at pH 6.5 and 30 °C. The steady-state kinetic data in LMPC, LMPG, and TDPC were collected by measuring DAGK activity (A) over a range of MgATP concentrations (0−8 mM) while keeping the concentration of DBG at a near-saturating concentration (20 mM) or (B) over a range of DBG concentrations (0−25 mM) while keeping the MgATP concentrations constant at a near-saturating concentration (3 mM). Each data point is the average of three measurements, and the resulting curves represent best fits by a modified form of the Michaelis−Menten equation in which a Hill coefficient was applied to the variable substrate concentration.

Circular Dichroism of DAGK in LMPC, LMPG, and TDPC Micelles. The secondary structure and aromatic side chain order of DAGK in LMPC, LMPG, and TDPC were probed using far- and near-UV CD spectroscopy, respectively. Data were collected at 45 °C and pH 6.5, the conditions used for NMR-based structural determination of DAGK (*26*). The far-UV CD spectra of DAGK in LMPC, LMPG, and TDPC show the strong negative bands at 208 and 222 nm characteristic of α-helical proteins and are very similar to the spectrum of DAGK in DPC (Figure 2A). From these spectra the percent α-helical content of DAGK in each of these detergents was calculated to be 79% (LMPC), 83% (LMPG), 79% (TDPC), and 69% (DPC). These values are all close to or within error of the 78% α-helicity observed in the NMR-determined structure of DAGK (*26*).

Near-UV CD spectroscopy provides information on the degree of structural order of aromatic side chains (*45*). It has previously been shown that when DAGK is unfolded, it exhibits no near-UV CD signal (*46*). As indicated in Figure 2B and in previous work (*46*), near-UV CD spectra of folded DAGK exhibit negative intensities indicating significant side chain order for at least some of its five Trp, three Phe, and two Tyr residues. Since most of DAGK's aromatic residues are believed to be located at or near the water−micelle interface rather than being either deeply buried or fully water-exposed, the near-UV CD spectra mostly report on side chain structural order at or near the water−micelle interface.

While the shapes of the spectra in Figure 2B are similar from detergent to detergent, the intensities vary dramatically, being much more intense for DAGK in lysophospholipids than in the alkylphosphocholine detergents. A reasonable interpretation of the data of Figure 2B is that the aromatic side chains of DAGK in the alkylphosphocholines generally exhibit a lower degree of structural order than in lysophospholipids, an observation that correlates with the relatively high activities observed for DAGK in the latter class of detergents. However, this correlation only holds within the structurally similar alkylphosphocholine and lysophospholipid series, as DAGK's spectrum in DM is similar in intensity to that in LMPC, even though DAGK's activity is DM is low (< 1 unit/mg).

Thermal Stability of DAGK in LMPC, LMPG, and TDPC Micelles. Wild-type DAGK's thermal stability was assessed by measuring its half-life for irreversible inactivation at elevated temperatures, a process previously examined in detail by Bowie and co-workers (*27*, *42*, *47*). Samples at pH 6.5 and 7.8 were incubated at 45 °C and at 70 °C. The data of Figure 3 led to the reported $t_{1/2}$ for activity loss presented in Table 3, which show that DAGK is much more stable at pH 6.5 than at pH 7.8.

DM micelles have been reported to maintain DAGK in a highly stable state (*27*, *48*) even though the enzyme exhibits only

Table 2: Steady-State Kinetic Parameters for DAGK Catalysis in Various Detergents

	DBG varied			MgATP varied		
detergent	$V_{max,DBG}$ (units/mg)	$K_{m,DBG}$ (mM)	$Hill_{DBG}$	$V_{max,ATP}$ (units/mg)	$K_{m,ATP}$ (mM)	$Hill_{ATP}$
LMPC	119 ± 6	4.7 ± 0.2	1.4	91 ± 5	0.5 ± 0.02	1.8
LMPG	50 ± 3	7.9 ± 0.4	1.6	46 ± 3	0.5 ± 0.02	1.5
TDPC	17 ± 1	8.8 ± 0.4	2.4	23 ± 2	1.4 ± 0.07	1.7
DM/CL[a]	ND	ND	ND	> 61 ± 8[a]	0.6 ± 0.1	1.0

[a]From ref *40*. These data were collected at fixed DBG = 10 mM, which most likely was not saturating. Therefore, this V_{max} is regarded as a lower limit to the true V_{max} when both substrate concentrations are saturating.

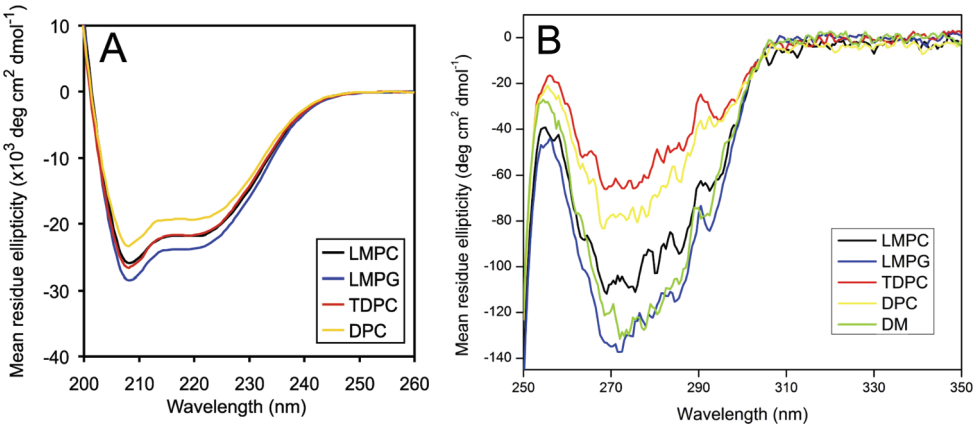

FIGURE 2: CD spectra of DAGK in micelles at pH 6.5 and 45 °C. Far-UV (A) and near-UV (B) CD spectra of DAGK were collected to assess the secondary structure and aromatic side chain order of DAGK, respectively, in LMPC (black), LMPG (blue), and TDPC (red). For comparison, spectra of DAGK in DPC are also included (yellow), as well as for DM (near-UV only, green). Analysis of this far-UV data led to the following estimates of secondary structure: LMPC, 79 ± 9% α-helix, 0% β-sheet, 21 ± 4% random coil; LMPG, 83 ± 8% α-helix, 0% β-sheet, 17 ± 4% random coil; TDPC, 79 ± 8% α-helix, 0% β-sheet, 20 ± 4% random coil; DPC, 69 ± 7% α-helix, 4 ± 1%, β-sheet, 27 ± 4% random coil.

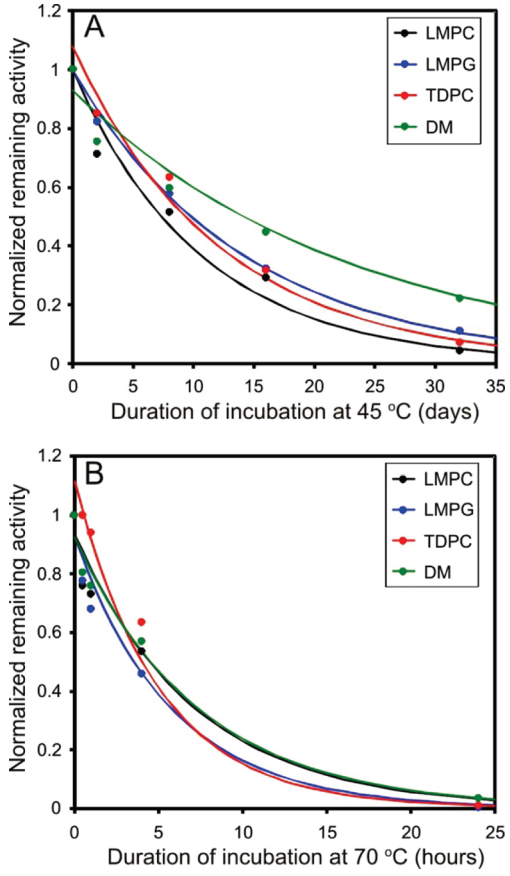

FIGURE 3: Irreversible loss of DAGK enzymatic activity with time during incubation at elevated temperatures. The stabilities of DAGK in LMPC (black), LMPG (blue), TDPC (red), and DM (green) were examined. The samples were prepared at pH 6.5 and incubated at either 45 °C (A) or 70 °C (B). Time point aliquots were removed and subjected to the standard DM/CL/DHG DAGK assay at 30 °C. The resulting data points were fit using Solver in Microsoft Excel to obtain the half-life for retention of DAGK.

very low activity in this detergent. At pH 6.5 DAGK's stability in LMPG, LMPC, and TDPC is comparable to its stability in DM, with $t_{1/2}$ ranging from several hours at 70 °C to 8−13 days at 45 °C (Table 3). That the enzyme is not significantly more resistant to heat inactivation in the new detergent systems than in

Table 3: Thermal Stability of DAGK in Different Micelles

	$t_{1/2}$ for irreversible loss of DAGK activity			
	pH 7.8		pH 6.5	
detergent	45 °C (days)	70 °C (h)	45 °C (days)	70 °C (h)
LMPC	1.3 ± 0.1	0.3 ± 0.02	8.0 ± 0.4	4.6 ± 0.3
LMPG	0.1 ± 0.01	0.1 ± 0.01	9.8 ± 0.5	3.5 ± 0.2
TDPC	0.7 ± 0.1	0.4 ± 0.02	10.1 ± 0.5	5.0 ± 0.3
DM	7.7 ± 0.4	0.7 ± 0.04	12.6 ± 0.7	5.1 ± 0.3

DM despite being more active in the new systems shows that there is no correlation within this set of detergents between DAGK activity and stability.

The temperature dependency of DAGK's far-UV CD spectra is shown in Figure 4, where only a minor loss of helicity is observed for LMPC, LMPG, and TDPC as the temperature is raised from 20 to 60 °C. Only above 60 °C does the helicity begin to drop steeply. In each case, when the temperature reaches 80 °C, DAGK has lost 18−23% of its α-helical content (Table 4). Most likely, this loss is due to melting of the N-terminal amphipathic helix, which encompasses about 20% of DAGK's helical content at 45 °C (*26*).

For LMPC and TDPC the loss of helicity observed in DAGK upon elevating the temperature to 80 °C was partially reversible, whereas in the case of LMPG reversibility is nearly complete (Table 4) although this detergent was not superior to the others in protecting against thermal inactivation (Table 3).

Near-UV CD spectra were also acquired as a function of temperature, which provides insight into aromatic side chain order (Figure 5). In the case of TDPC the data resemble the corresponding far-UV CD data in that there is little change until ca. 60 °C, above which signal intensity is steeply reduced until it reaches baseline near 80 °C. For LMPG and LMPC there are significant reductions in the far-UV CD signal intensity as the temperature is raised, with baseline in both cases being reached by 80 °C. However, for the LMPC case reductions in signal intensity become much steeper when 60 °C is exceeded. We speculate that DAGK in lysophospholipids below 60 °C possesses a class of side chain conformational order that is absent in TDPC even at low temperatures, which may be related to the lower

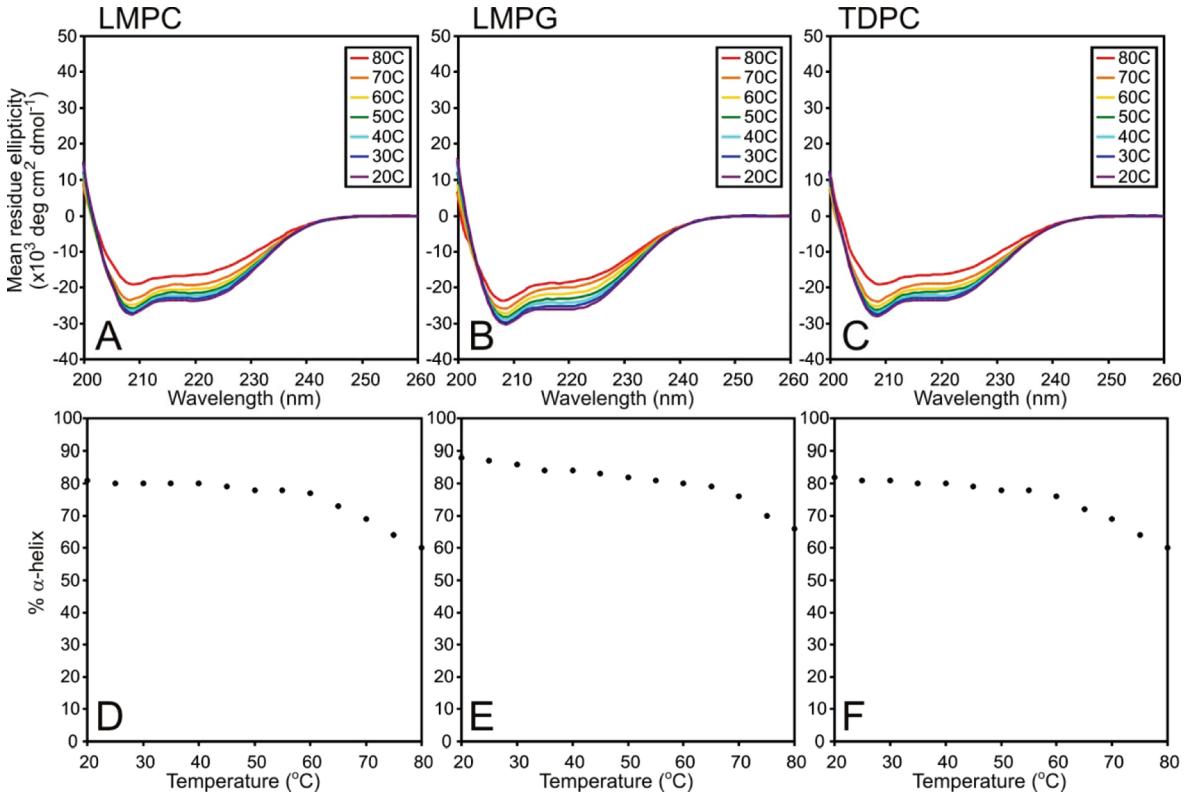

FIGURE 4: Assessment of helix stability in DAGK by monitoring the temperature dependence of the far-UV CD spectrum of DAGK in LMPC, LMPG, and TDPC micelles at pH 6.5.

Table 4: Percent α-Helix of DAGK at pH 6.5 Determined from Far-UV CD Spectra Acquired Successively at 20 °C, 80 °C, and after Return to 20 °C

detergent	20 °C	80 °C	20 °C (after heating)
LMPC	81 ± 8	60 ± 6	74 ± 7
LMPG	88 ± 8	66 ± 6	85 ± 9
TDPC	82 ± 8	59 ± 7	72 ± 7

catalytic activity of DAGK observed in TDPC relative to the lysophospholipids. At 60 °C, DAGK has lost this class of side chain order in all three detergents tested but still retains a second class of side chain order. For all three detergents this remaining side chain order is lost by the point 80 °C is reached, which likely corresponds with complete loss of stable tertiary structure.

Unlike the case for the far-UV CD data, we found that returning the temperature to 20 °C in no case allowed DAGK to recapitulate its original near-UV CD spectrum (data not shown), indicating that the loss of tertiary structural order is not reversible. This is consistent with the previous observations of Bowie and co-workers (*47*).

TROSY NMR Spectra of DAGK in LMPC, LMPG, and TDPC Micelles. ^{15}N-TROSY-HSQC spectra were acquired at 45 °C for pH 6.5 samples of WT DAGK in LMPC, LMPG, TDPC, and DPC micelles (Figure 6). Overall, the spectra are generally similar and exhibit the modest spectral dispersion that is usually associated with helical membrane proteins. However, while the quality of the spectra in LMPG and TDPC is high (approaching that observed in DPC) the LMPC spectrum exhibits fewer peaks. This is not because there are many missing peaks; rather, it is because at the peak plotting level used (which is comparable for all four spectra) many LMPC peaks are broadened to the point where their maxima fall below the plotting level threshold. There are several possible sources for the line broadening. One possibility is that DAGK−LMPC mixed micelles are larger than the corresponding DAGK−TDPC and DAGK−LMPG micelles. Another possible contribution to line broadening is the presence of internal conformational motions for DAGK in LMPC micelles that are intermediate on the NMR time scale, leading to exchange broadening. A final possible contributing factor is conformational microheterogeneity that results in many similar but nonidentical/nonexchanging superimposed peaks. Additional experiments would be required to determine which of the above phenomena are the actual contributing factors.

The quality of the DAGK spectra from TDPC and LMPG is excellent for a 40 kDa homotrimeric multispan membrane protein as part of a much larger micellar complex. The average line idth of the peaks seen in each of these detergents is 25 Hz. The TDPC and LMPG spectra are similar but are also sufficiently *different* from each other and from the assigned DPC spectrum such that the assignments that are available for the DPC peaks (*30*) cannot in many cases be reliably extrapolated to the TDPC and LMPG cases. The differences in specific peak positions may be explained by the fact that the detergent−DAGK interface is quite extensive, such that variations in the covalent structure of each detergent result in modest but widespread changes in resonance position.

NOESY NMR Data Show Differences in DAGK−Detergent Interactions for DPC versus LMPC. 3-D ^{1}H,^{15}N-NOESY-TROSY NMR spectra were acquired for U-^{15}N-DAGK in both DPC and LMPC micelles. We used the "half-filtered" version of this 3-D experiment, which leads to NOE cross-peaks being observed for pairs of proximal protons for which at least one of the two interacting protons is directly attached to ^{15}N. In analyzing these data we focused on NOEs between the tryptophan side chain indole NH proton and detergent protons, observation of which can be taken as an indication of at least

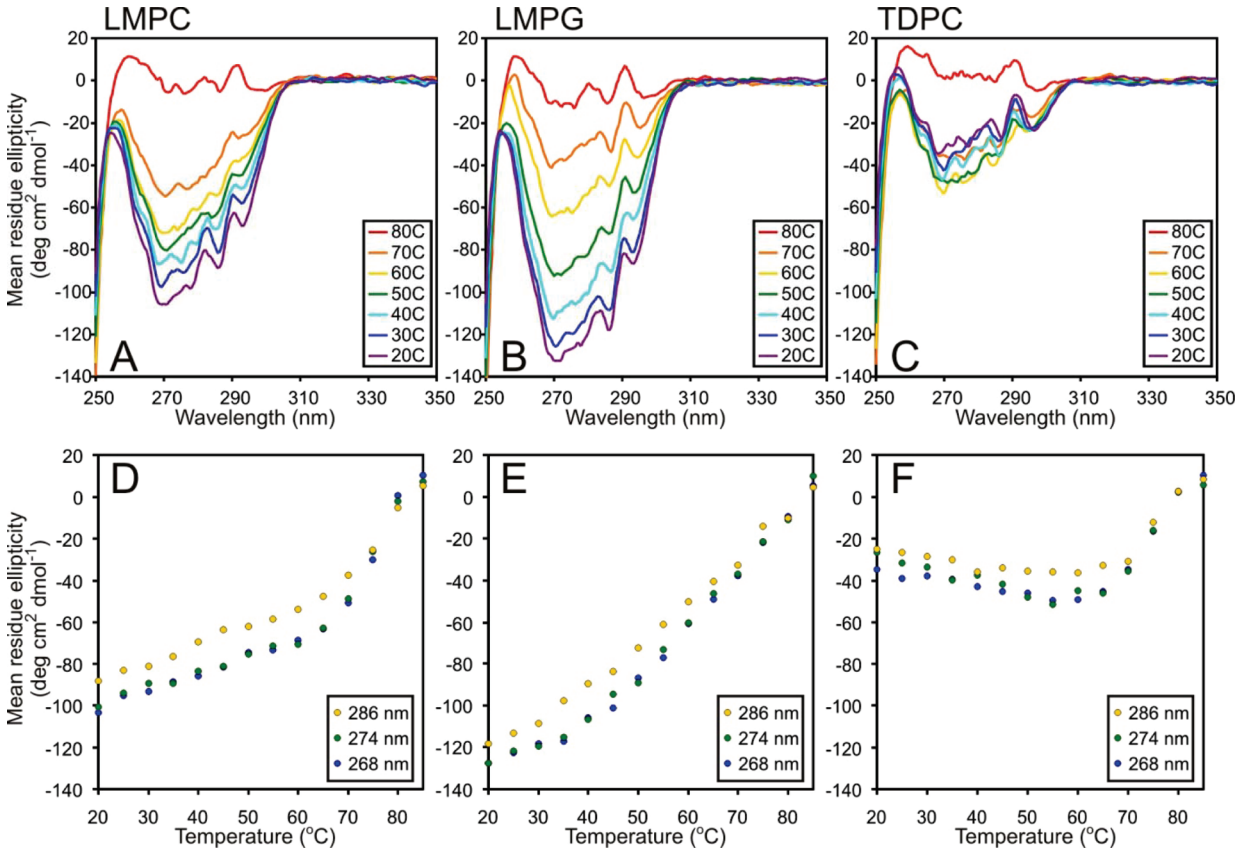

FIGURE 5: Use of near-UV CD to assess aromatic side chain order in DAGK as a function of temperature at pH 6.5. The ellipticity values at 268, 274, and 286 nm correspond to absorbance maxima for phenylalanine, tyrosine, and tryptophan side chains, respectively.

transient proximity (< 5 Å) between the indole proton and protons on the detergent.[2]

Figure 7 shows 2-D strip plots from the ^{1}H,^{15}N-NOESY data that illustrate the NOEs observed between the indole protons and the detergents. In the case of DPC (Figure 7A), it is seen that strong NOEs are observed between all indole NH protons and both choline methyl (3.3 ppm) and alkyl chain protons (1.4 ppm). That NOEs to these spatially distinct parts of DPC are simultaneously observed undoubtably reflects both the high heterogeneity of detergent−membrane protein interactions (at any given snapshot) and also the highly dynamic nature of these interactions. These data indicate that, on the average, the Trp side chains of DAGK in DPC micelles spend as much time near the charged choline headgroup as they do with the hydrophobic micelle interior. In the case of LMPC, a significantly different pattern is seen (Figure 7B). While strong NOEs are observed between protons from the acyl chain (1.4 ppm) and the indole peaks, NOEs between the indoles and the choline headgroup are weak or absent. Some NOEs are observed between protons from the glycerol backbone (3.8−4.25 ppm) and the indoles, although these are not as strong as the NOEs to the acyl chain. These results indicate that average position of the indole side chain in LMPC micelles is significantly deeper (toward the apolar micellar interior) than in the case of DPC, such that direct indole/choline interactions are largely avoided in the former case. The Trp side chains are not so deeply buried, however, that NOEs are observed between the indole NH and the terminal methyl group of the aliphatic chain in LMPC, consistent with the Trp side chains being restrained so as to avoid the center of the micelles.

[2]For this study the focus is limited to indole−detergent NOEs because the side chains of other amino acids in DAGK have proven very difficult to detect or assign (even according to amino acid type; see refs *1* and *2* for a description of the nature of the difficulties). Second, while backbone amide proton resonance assignments are available for DAGK in DPC (*3*), this is not yet the case for the enzyme in LMPC micelles.

DISCUSSION

Early work on *E. coli* DAGK focused on the catalytic properties of this enzyme under conditions in which it was solubilized using Triton X-100 or alkyl glycoside detergents (*21*−*25*). Under these conditions DAGK was found to require the presence of added phospholipid in order to exhibit significant catalytic activity. This led to the notion that lipids play a requisite "cofactor" role in promoting DAGK's catalytic activity. The present work shows that the C_{14}-based detergents LMPC, LMPG, and TDPC were able to sustain specific DAGK activities of at least 10 units/mg under standard assay conditions. Of these, LMPC yielded the highest activity (66 units/mg), with the C_{12} and C_{16} analogues of this detergent also sustaining > 10 units/mg. Indeed, the V_{max} for DAGK in LMPC, LMPG, and TDPC micelles was seen to be roughly 100, 50, and 20 units/mg, respectively, with the 100 units/mg observed for DAGK in LMPC being roughly the same as the highest activities previously observed for the enzyme in mixed micellar, bicellar, or vesicular conditions (*3*, *31*, *43*, *44*, *49*).

There appear to be three key factors that promote DAGK activity. First, the C_{14} chain was found to be superior to either shorter or longer chains. Most likely, the diameter of micelles containing C_{14} chains is an optimal match for the hydrophobic span of the transmembrane domain of DAGK. While the diameters of LMPC and LMPG micelles have not been directly measured, from studies (*50*−*53*) of C_{16}-lyso-PG and C_{8-12}-lyso-PC, it is possible to estimate that the span of the hydrophobic

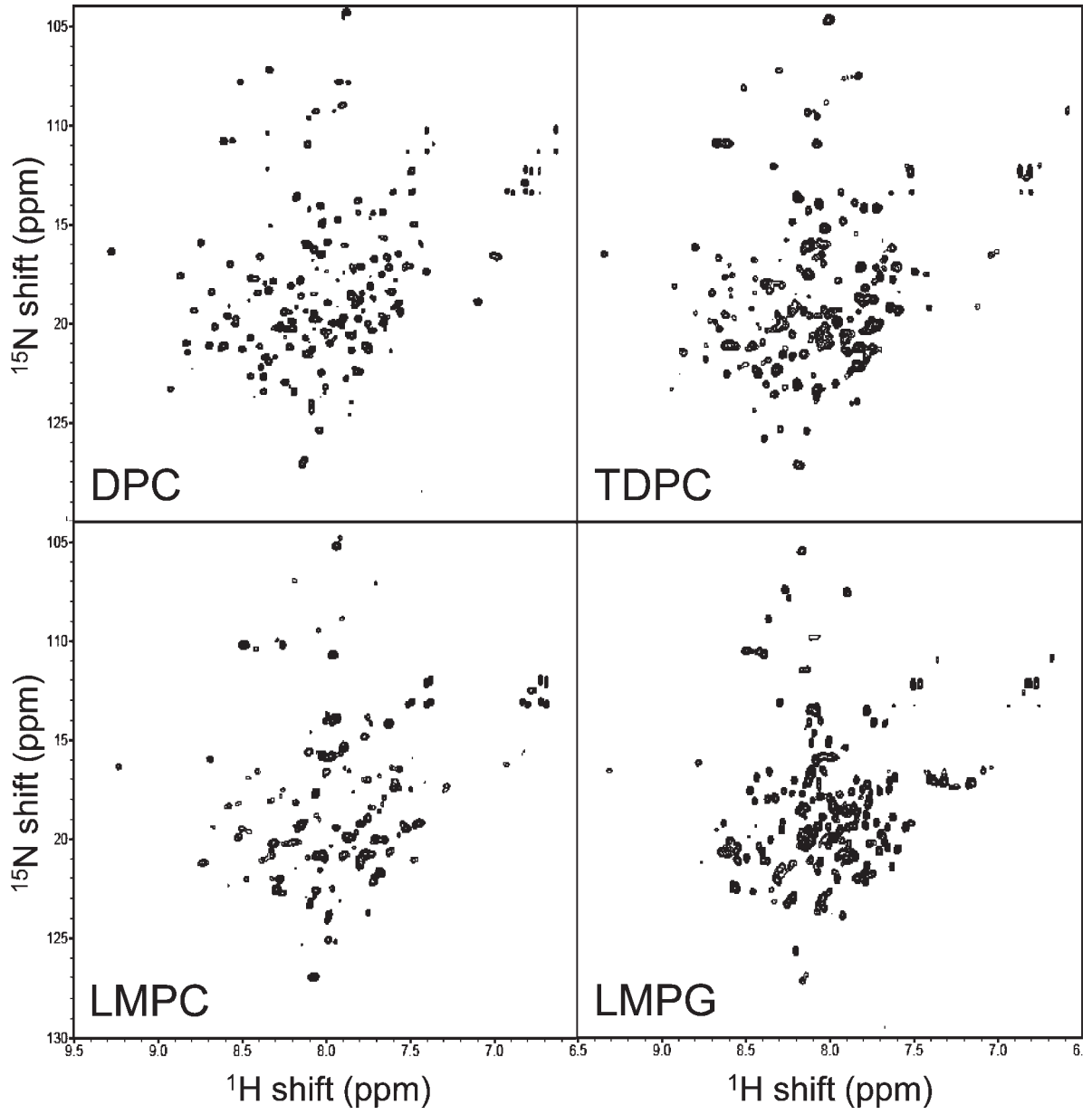

FIGURE 6: 800 MHz ^{15}N-TROSY spectra of DAGK in LMPC, LMPG, DPC, and TDPC micelles at 45 °C. The samples in TDPC and LMPG contained 10 mM Bis-Tris, 2 mM magnesium chloride, 0.5 mM EDTA, and 10% (v/v) D_2O, pH 6.5. The samples in DPC and LMPC contained 250 mM imidazole, 0.5 mM EDTA, and 10% (v/v) D_2O, pH 6.5.

domain of LMPG and LMPC micelles is in the range of 30−35 Å, with the thickness of the glycerol backbone/headgroup domain being roughly 10−12 Å on each side. Lee and co-workers have examined DAGK's activity in a series of lipid vesicles composed of phosphatidylcholine with two monounsaturated chains and found that the enzyme is most active in di($C_{18:1}$)-PC vesicles (*44*), which have a hydrophobic span of 30 Å, roughly the same as estimated for LMPC and LMPG micelles. This appears to be a good match to the observed hydrophobic span of the experimental DAGK structure (*26*), which is 30−33 Å. This highlights the importance of appropriate matching of the transmembrane span of a membrane protein with the thickness of the membrane or membrane-mimetic in which it sits to optimize protein structure, stability, and function, as others have previously described (*54*−*58*).

A second key factor in promoting activity appears to be the presence of the glycerol spacer between the acyl chain and the charged headgroup, as reflected by the higher activities observed in the lysophospholipids relative to the alkylphosphocholines. The glycerol spacer/backbone is, of course, present in the glycerophospholipids that dominate the composition of the plasma membrane of *E. coli*. It is also interesting to note that the lysophospholipids are the only commercially available class of single-chain ionic detergents that has a polar-but-uncharged spacer between the apolar tail and the charged headgroup. Our results suggest that DAGK has evolved so as to prefer the presence of a glycerol spacer over an abrupt chain-to-headgroup transition. This may be a property shared by many other membrane proteins. Other recent studies have highlighted some of the advantages of working with lysophospholipids as detergents (*59*−*61*), which seem to particularly effective at sustaining high membrane protein solubility without disrupting structure and function (*62*−*65*).

Finally, DAGK exhibited a preference for the zwitterionic phosphocholine headgroup of LMPC over the anionic headgroup of LMPG. This result is strikingly similar to results for DAGK activity in lipid vesicles, where Lee et al. observed DAGK

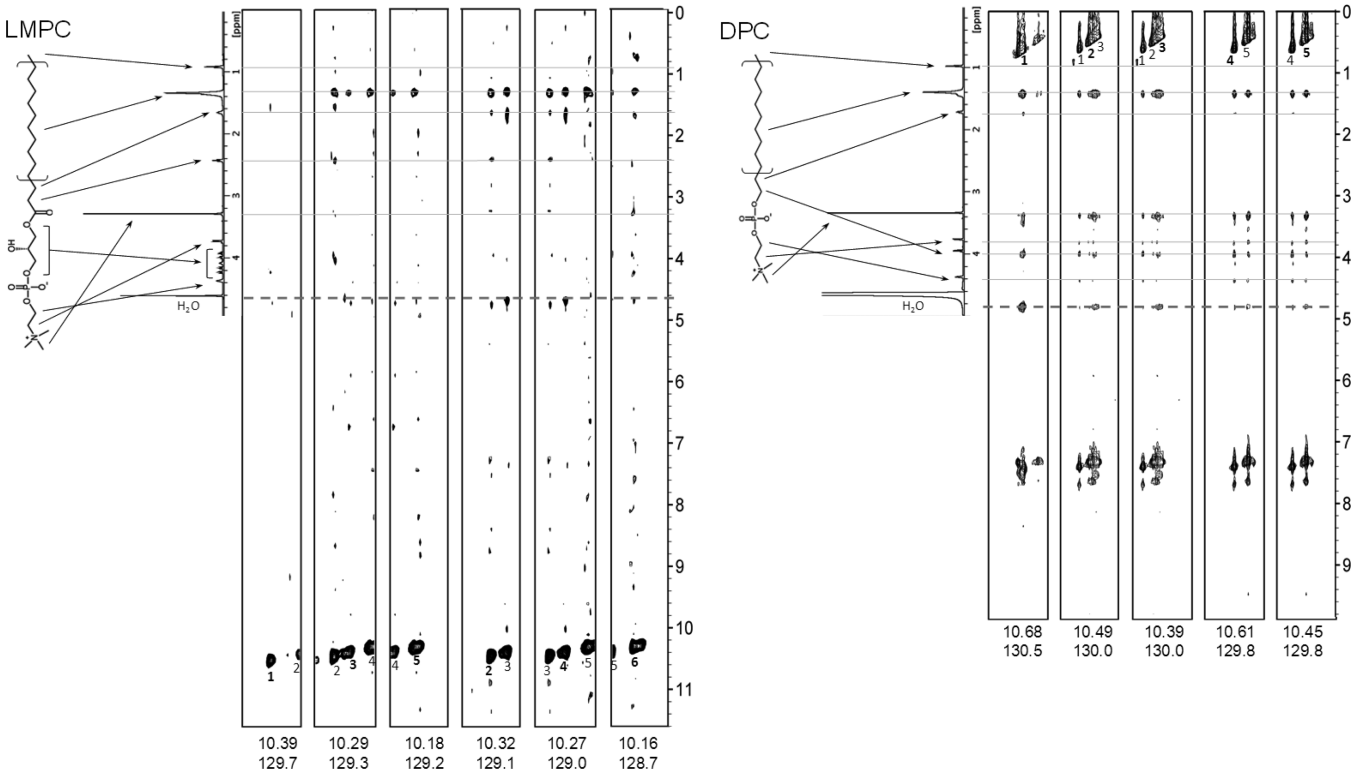

FIGURE 7: 2-D strip plots showing NOEs to the tryptophan indole NH protons from 3-D $^{1}H-^{15}N$-NOESY-TROSY spectra collected for U-^{15}N-DAGK in DPC (A) and LMPC (B) micelles at 800 MHz and 45 °C. Associated with each set of strips is a 1-D NMR spectrum for pure DPC and LMPC showing resonance assignments. In the strip plots for the DPC case (A) the indole NH proton diagonal peaks appear upfield of the rest of the spectrum rather than in the expected 9.5−10.5 ppm range because the peaks are "aliased" as a result of being outside of the spectral window of the TPPI/States-based NMR experiment used to acquire these data (*39*). In the LMPC case (B) the peaks appear at the expected chemical shifts because they fell within the observation sweep width. In the LMPC case, side chain-perdeuterated DAGK was used, which is why NOEs between the NH indole protons to their two nearest neighbors on the indole rings are not observed at 7.2−7.8 ppm, unlike the DPC case where DAGK was not deuterated and these NOEs are quite pronounced.

to be most active in phosphatidylcholine vesicles compared to vesicles composed of phosphatidylglycerol or phosphatidylethanolamine (*42*). This is despite the fact that *E. coli* membranes are bereft of phosphatidylcholine but are rich in phosphatidylglycerol and phosphatidylethanolamine (*66*). Given that DAGK actually shows a preference for anionic lipids as activators when lipids are added to neutral detergent micelles (*24*, *25*), it is seems likely the anionic charge density present in LMPG micelles represents "too much of a good thing" from DAGK's standpoint. We have not yet tested DAGK's activity in LMPC/LMPG mixtures. In any case, charge alone is not the only important property of the detergent headgroup, as illustrated by the fact that the zwitterionic Z3-14 and ASB-14 did not support DAGK activity. This is possibly because the orientation of the positive and negative charge with respect to the main chain is reversed in these compounds relative to the phosphocholine detergents and virtually all known natural zwitterionic phospholipids.

The most important insight regarding how LMPC, LMPG, and TDPC may promote DAGK's catalytic activity relative to DPC is provided by NOE measurements (Figure 7). These results indicate that the Trp side chains of DAGK in both DPC and LMPC micelles interact strongly with the detergent aliphatic chains but avoid contacts with the chain termini, which are found primarily in the center of the micelles. This is as expected for Trp side chains based both on the structure of DAGK (*26*) and on the observation that Trp side chains are usually found in the membrane bilayer, but fairly near the surface. However, the NOE data also show that while the Trp side chains of DAGK in LMPC interact almost exclusively with the aliphatic groups and, to a lesser extent, the glycerol spacer, the situation is very different in DPC. Namely, strong NOE interactions are observed between the indole rings with the choline methyl protons located at the end of the headgroup. Apparently, in the absence of the glycerol spacer present in both LMPC and in most lipids of native membranes the indole side chains are forced to come in frequent contact with the most polar parts of the micelle. We suggest that it is this inappropriate contact, perhaps compounded by hydrophobic mismatch, that results in the reduction in the aromatic side chain order evident in the near-UV CD spectrum of DAGK in DPC relative to LMPC conditions, as well as DAGK's lower activity and stability in DPC micelles.

Our conclusions that micelles comprised of certain C_{14} detergents can sustain DAGK in a stable and nearly fully active form and that these detergents also lead to high-quality NMR spectra may be very important for future structural studies of this enzyme. While the structure of the substrate-free form of DAGK was recently determined in DPC micelles, the K_m of the enzyme for MgATP and diacylglycerol are significantly elevated, to the point where structural studies of saturated DAGK−substrate complexes may be very difficult, particularly for complexes that include diacylglycerol. The results of this paper establish that in LMPC and LMPG the K_m for DAGK's substrates are close to their values under ideal conditions and are low enough such that structural studies of saturated binary and ternary complexes using NMR methods are now feasible. This is an important development. While DAGK has previously been shown to be fully active in lipid vesicles (*3*), bicelles (*3*), lipid−detergent mixed micelles (*3*, *31*), and even amphipols (*40*), these alternative

membrane-mimetic media have not yet yielded either high-quality NMR spectra or well-diffracting crystals of this enzyme.

CONCLUSIONS

Great care must be exercised when working with membrane proteins in micelles to ensure that potential detergent-induced perturbations of native-like structural or functional properties are taken into account. However, the success of LMPC in sustaining DAGK's high thermal stability and catalytic activity highlights the fact that for at least some integral membrane proteins the best available detergents appear to exert only very modest perturbations. This is fortunate because some biophysical and biochemical methods are easier to carry out in detergent solutions than in more complex membrane-mimetic media such as bicelles, nanodisks, lipidic cubic phases, or unilamellar vesicles. The fact that lysophospholipids appear to be well suited for DAGK appears to be closely related to the fact that they are the only class of single-chain detergents that resembles the majority of phospholipids found in nature in that they have a polar-but-uncharged (glycerol) spacer that links the apolar tail to the charged headgroup. The lysophospholipids may be worthy of much more widespread use in membrane protein research.

ACKNOWLEDGMENT

The authors thank Megan Wadington for carrying out some of the early experimental measurements of this work and Stanley C. Howell for useful discussion and NMR technical assistance.

REFERENCES

1. Kim, H. J., Howell, S. C., Van Horn, W. D., Jeon, Y. H., and Sanders, C. R. (2009) Recent advances in the application of solution NMR spectroscopy to multi-span integral membrane proteins. *Prog. Nucl. Magn. Reson. Spectrosc. 55*, 335–360.
2. Sanders, C. R., and Sonnichsen, F. (2006) Solution NMR of membrane proteins: practice and challenges. *Magn. Reson. Chem. 44* (Spec. No.), S24–S40.
3. Czerski, L., and Sanders, C. R. (2000) Functionality of a membrane protein in bicelles. *Anal. Biochem. 284*, 327–333.
4. Hanson, M. A., Cherezov, V., Griffith, M. T., Roth, C. B., Jaakola, V. P., Chien, E. Y., Velasquez, J., Kuhn, P., and Stevens, R. C. (2008) A specific cholesterol binding site is established by the 2.8 Å structure of the human beta2-adrenergic receptor. *Structure 16*, 897–905.
5. Hunte, C., and Richers, S. (2008) Lipids and membrane protein structures. *Curr. Opin. Struct. Biol. 18*, 406–411.
6. Qin, L., Sharpe, M. A., Garavito, R. M., and Ferguson-Miller, S. (2007) Conserved lipid-binding sites in membrane proteins: a focus on cytochrome *c* oxidase. *Curr. Opin. Struct. Biol. 17*, 444–450.
7. Reichow, S. L., and Gonen, T. (2009) Lipid-protein interactions probed by electron crystallography. *Curr. Opin. Struct. Biol. 19*, 560–565.
8. Choowongkomon, K., Carlin, C. R., and Sonnichsen, F. D. (2005) A structural model for the membrane-bound form of the juxtamembrane domain of the epidermal growth factor receptor. *J. Biol. Chem. 280*, 24043–24052.
9. Chou, J. J., Kaufman, J. D., Stahl, S. J., Wingfield, P. T., and Bax, A. (2002) Micelle-induced curvature in a water-insoluble HIV-1 Env peptide revealed by NMR dipolar coupling measurement in stretched polyacrylamide gel. *J. Am. Chem. Soc. 124*, 2450–2451.
10. Kang, C., Tian, C., Sonnichsen, F. D., Smith, J. A., Meiler, J., George, A. L., Jr., Vanoye, C. G., Kim, H. J., and Sanders, C. R. (2008) Structure of KCNE1 and implications for how it modulates the KCNQ1 potassium channel. *Biochemistry 47*, 7999–8006.
11. Lee, S. Y., Lee, A., Chen, J., and MacKinnon, R. (2005) Structure of the KvAP voltage-dependent K^+ channel and its dependence on the lipid membrane. *Proc. Natl. Acad. Sci. U.S.A. 102*, 15441–15446.
12. MacKenzie, K. R., and Fleming, K. G. (2008) Association energetics of membrane spanning alpha-helices. *Curr. Opin. Struct. Biol. 18*, 412–419.
13. Matthews, E. E., Zoonens, M., and Engelman, D. M. (2006) Dynamic helix interactions in transmembrane signaling. *Cell 127*, 447–450.
14. Mi, L. Z., Grey, M. J., Nishida, N., Walz, T., Lu, C., and Springer, T. A. (2008) Functional and structural stability of the epidermal growth factor receptor in detergent micelles and phospholipid nanodiscs. *Biochemistry 47*, 10314–10323.
15. Faham, S., and Bowie, J. U. (2002) Bicelle crystallization: a new method for crystallizing membrane proteins yields a monomeric bacteriorhodopsin structure. *J. Mol. Biol. 316*, 1–6.
16. Nath, A., Atkins, W. M., and Sligar, S. G. (2007) Applications of phospholipid bilayer nanodiscs in the study of membranes and membrane proteins. *Biochemistry 46*, 2059–2069.
17. Popot, J. L. (2010) Amphipols, nanodiscs, and fluorinated surfactants: three nonconventional approaches to studying membrane proteins in aqueous solutions, *Annu. Rev. Biochem.* (in press).
18. Prive, G. G. (2009) Lipopeptide detergents for membrane protein studies. *Curr. Opin. Struct. Biol. 19*, 379–385.
19. Prosser, R. S., Evanics, F., Kitevski, J. L., and Al-Abdul-Wahid, M. S. (2006) Current applications of bicelles in NMR studies of membrane-associated amphiphiles and proteins. *Biochemistry 45*, 8453–8465.
20. Sanders, C. R., Kuhn, H. A., Gray, D. N., Keyes, M. H., and Ellis, C. D. (2004) French swimwear for membrane proteins. *ChemBioChem 5*, 423–426.
21. Bohnenberger, E., and Sandermann, H., Jr. (1983) Lipid dependence of diacylglycerol kinase from *Escherichia coli*. *Eur. J. Biochem. 132*, 645–650.
22. Russ, E., Kaiser, U., and Sandermann, H., Jr. (1988) Lipid-dependent membrane enzymes. Purification to homogeneity and further characterization of diacylglycerol kinase from *Escherichia coli*. *Eur. J. Biochem. 171*, 335–342.
23. Schneider, E. G., and Kennedy, E. P. (1976) Partial purification and properties of diglyceride kinase from *Escherichia coli*. *Biochim. Biophys. Acta 441*, 201–212.
24. Walsh, J. P., and Bell, R. M. (1986) *sn*-1,2-Diacylglycerol kinase of *Escherichia coli*. Structural and kinetic analysis of the lipid cofactor dependence. *J. Biol. Chem. 261*, 15062–15069.
25. Walsh, J. P., and Bell, R. M. (1986) *sn*-1,2-Diacylglycerol kinase of *Escherichia coli*. Mixed micellar analysis of the phospholipid cofactor requirement and divalent cation dependence. *J. Biol. Chem. 261*, 6239–6247.
26. Van Horn, W. D., Kim, H. J., Ellis, C. D., Hadziselimovic, A., Sulistijo, E. S., Karra, M. D., Tian, C., Sonnichsen, F. D., and Sanders, C. R. (2009) Solution nuclear magnetic resonance structure of membrane-integral diacylglycerol kinase. *Science 324*, 1726–1729.
27. Zhou, Y., and Bowie, J. U. (2000) Building a thermostable membrane protein. *J. Biol. Chem. 275*, 6975–6979.
28. Miller, K. J., McKinstry, M. W., Hunt, W. P., and Nixon, B. T. (1992) Identification of the diacylglycerol kinase structural gene of *Rhizobium meliloti* 1021. *Mol. Plant−Microbe Interact. 5*, 363–371.
29. Oxenoid, K., Sonnichsen, F. D., and Sanders, C. R. (2002) Topology and secondary structure of the N-terminal domain of diacylglycerol kinase. *Biochemistry 41*, 12876–12882.
30. Oxenoid, K., Kim, H. J., Jacob, J., Sonnichsen, F. D., and Sanders, C. R. (2004) NMR assignments for a helical 40 kDa membrane protein. *J. Am. Chem. Soc. 126*, 5048–5049.
31. Badola, P., and Sanders, C. R. (1997) *Escherichia coli* diacylglycerol kinase is an evolutionarily optimized membrane enzyme and catalyzes direct phosphoryl transfer. *J. Biol. Chem. 272*, 24176–24182.
32. Walsh, J. P., Fahrner, L., and Bell, R. M. (1990) *sn*-1,2-Diacylglycerol kinase of *Escherichia coli*. Diacylglycerol analogues define specificity and mechanism. *J. Biol. Chem. 265*, 4374–4381.
33. Riek, R., Pervushin, K., and Wuthrich, K. (2000) TROSY and CRINEPT: NMR with large molecular and supramolecular structures in solution. *Trends Biochem. Sci. 25*, 462–468.
34. Weigelt, J. (1998) Single scan, sensitivity- and gradient-enhanced TROSY for multidimensional NMR experiments. *J. Am. Chem. Soc. 120*, 10778–10779.
35. Delaglio, F., Grzesiek, S., Vuister, G. W., Zhu, G., Pfeifer, J., and Bax, A. (1995) NMRPipe: a multidimensional spectral processing system based on UNIX pipes. *J. Biomol. NMR 6*, 277–293.
36. Czisch, M., and Boelens, R. (1998) Sensitivity enhancement in the TROSY experiment. *J. Magn. Reson. 134*, 158–160.
37. Salzmann, M., Pervushin, K., Wider, G., Senn, H., and Wuthrich, K. (1998) TROSY in triple-resonance experiments: new perspectives for sequential NMR assignment of large proteins. *Proc. Natl. Acad. Sci. U.S.A. 95*, 13585–13590.
38. Zhu, G., Kong, X. M., and Sze, K. H. (1999) Gradient and sensitivity enhancement of 2D TROSY with water flip-back, 3D NOESY-TROSY and TOCSY-TROSY experiments. *J. Biomol. NMR 13*, 77–81.

39. Schulte-Herbruggen, T., Briand, J., Meissner, A., and Sorensen, O. W. (1999) Spin-state-selective TPPI: a new method for suppression of heteronuclear coupling constants in multidimensional NMR experiments. *J. Magn. Reson. 139*, 443–446.
40. Gorzelle, B. M., Hoffman, A. K., Keyes, M. H., Gray, D. N., Ray, D. G., and Sanders, C. R. (2002) Amphipols can support the activity of a membrane enzyme. *J. Am. Chem. Soc. 124*, 11594–11595.
41. Vinogradova, O., Sonnichsen, F., and Sanders, C. R. (1998) On choosing a detergent for solution NMR studies of membrane proteins. *J. Biomol. NMR 11*, 381–386.
42. Lau, F. W., Nauli, S., Zhou, Y., and Bowie, J. U. (1999) Changing single side-chains can greatly enhance the resistance of a membrane protein to irreversible inactivation. *J. Mol. Biol. 290*, 559–564.
43. Pilot, J. D., East, J. M., and Lee, A. G. (2001) Effects of phospholipid headgroup and phase on the activity of diacylglycerol kinase of Escherichia coli. *Biochemistry 40*, 14891–14897.
44. Pilot, J. D., East, J. M., and Lee, A. G. (2001) Effects of bilayer thickness on the activity of diacylglycerol kinase of *Escherichia coli*. *Biochemistry 40*, 8188–8195.
45. Rogers, D. M., and Hirst, J. D. (2004) First-principles calculations of protein circular dichroism in the near ultraviolet. *Biochemistry 43*, 11092–11102.
46. Nagy, J. K., Lonzer, W. L., and Sanders, C. R. (2001) Kinetic study of folding and misfolding of diacylglycerol kinase in model membranes. *Biochemistry 40*, 8971–8980.
47. Zhou, Y., Lau, F. W., Nauli, S., Yang, D., and Bowie, J. U. (2001) Inactivation mechanism of the membrane protein diacylglycerol kinase in detergent solution. *Protein Sci. 10*, 378–383.
48. Li, Q., Mittal, R., Huang, L., Travis, B., and Sanders, C. R. (2009) Bolaamphiphile-class surfactants can stabilize and support the function of solubilized integral membrane proteins. *Biochemistry 48*, 11606–11608.
49. Lau, F. W., Chen, X., and Bowie, J. U. (1999) Active sites of diacylglycerol kinase from *Escherichia coli* are shared between subunits. *Biochemistry 38*, 5521–5527.
50. Chou, J. J., Baber, J. L., and Bax, A. (2004) Characterization of phospholipid mixed micelles by translational diffusion. *J. Biomol. NMR 29*, 299–308.
51. Lipfert, J., Columbus, L., Chu, V. B., Lesley, S. A., and Doniach, S. (2007) Size and shape of detergent micelles determined by small-angle X-ray scattering. *J. Phys. Chem. B 111*, 12427–12438.
52. Mendz, G. L., Jamie, I. M., and White, J. W. (1992) Effects of acyl chain length on the conformation of myelin basic protein bound to lysolipid micelles. *Biophys. Chem. 45*, 61–77.
53. Vitiello, G., Ciccarelli, D., Ortona, O., and D'Errico, G. (2009) Microstructural characterization of lysophosphatidylcholine micellar aggregates: the structural basis for their use as biomembrane mimics. *J. Colloid Interface Sci. 336*, 827–833.
54. Botelho, A. V., Huber, T., Sakmar, T. P., and Brown, M. F. (2006) Curvature and hydrophobic forces drive oligomerization and modulate activity of rhodopsin in membranes. *Biophys. J. 91*, 4464–4477.
55. Columbus, L., Lipfert, J., Jambunathan, K., Fox, D. A., Sim, A. Y., Doniach, S., and Lesley, S. A. (2009) Mixing and matching detergents for membrane protein NMR structure determination. *J. Am. Chem. Soc. 131*, 7320–7326.
56. Holt, A., and Killian, J. A. (2010) Orientation and dynamics of transmembrane peptides: the power of simple models. *Eur. Biophys. J. 39*, 609–621.
57. Lee, A. G. (2003) Lipid-protein interactions in biological membranes: a structural perspective. *Biochim. Biophys. Acta 1612*, 1–40.
58. Soubias, O., Niu, S. L., Mitchell, D. C., and Gawrisch, K. (2008) Lipid-rhodopsin hydrophobic mismatch alters rhodopsin helical content. *J. Am. Chem. Soc. 130*, 12465–12471.
59. Beel, A. J., Mobley, C. K., Kim, H. J., Tian, F., Hadziselimovic, A., Jap, B., Prestegard, J. H., and Sanders, C. R. (2008) Structural studies of the transmembrane C-terminal domain of the amyloid precursor protein (APP): does APP function as a cholesterol sensor? *Biochemistry 47*, 9428–9446.
60. Krueger-Koplin, R. D., Sorgen, P. L., Krueger-Koplin, S. T., Rivera-Torres, I. O., Cahill, S. M., Hicks, D. B., Grinius, L., Krulwich, T. A., and Girvin, M. E. (2004) An evaluation of detergents for NMR structural studies of membrane proteins. *J. Biomol. NMR 28*, 43–57.
61. Tian, C., Vanoye, C. G., Kang, C., Welch, R. C., Kim, H. J., George, A. L., Jr., and Sanders, C. R. (2007) Preparation, functional characterization, and NMR studies of human KCNE1, a voltage-gated potassium channel accessory subunit associated with deafness and long QT syndrome. *Biochemistry 46*, 11459–11472.
62. Aiyar, N., Nambi, P., Stassen, F., and Crooke, S. T. (1987) Solubilization and reconstitution of vasopressin V1 receptors of rat liver. *Mol. Pharmacol. 32*, 34–36.
63. Aiyar, N., Bennett, C. F., Nambi, P., Valinski, W., Angioli, M., Minnich, M., and Crooke, S. T. (1989) Solubilization of rat liver vasopressin receptors as a complex with a guanine-nucleotide-binding protein and phosphoinositide-specific phospholipase C. *Biochem. J. 261*, 63–70.
64. Aiyar, N., Valinski, W., Nambi, P., Minnich, M., Stassen, F. L., and Crooke, S. T. (1989) Solubilization of a guanine nucleotide-sensitive form of vasopressin V2 receptors from porcine kidney. *Arch. Biochem. Biophys. 268*, 698–706.
65. Huang, P., Liu, Q., and Scarborough, G. A. (1998) Lysophosphatidylglycerol: a novel effective detergent for solubilizing and purifying the cystic fibrosis transmembrane conductance regulator. *Anal. Biochem. 259*, 89–97.
66. Shibuya, I. (1992) Metabolic regulations and biological functions of phospholipids in *Escherichia coli*. *Prog. Lipid Res. 31*, 245–299.